

# Measurement of the angular resolution of the ARGO-YBJ detector

G. Di Sciascio and E. Rossi for the ARGO-YBJ Collaboration  
INFN, sez. di Napoli and Dip. di Scienze Fisiche dell'Università, Napoli, Italy

Email: giuseppe.disciascio@na.infn.it, elvira.rossi@na.infn.it

**Abstract**—The ARGO-YBJ experiment is almost completely installed at the YangBaJing Cosmic Ray Laboratory (Tibet, P.R. China, 4300 m a.s.l.). We present the first results on the angular resolution measured with increasing portions of the full detector. The comparison of experimental results with MC simulations is discussed.

## I. INTRODUCTION

The ARGO-YBJ detector is constituted by a single layer of Resistive Plate Chambers (RPCs) with  $\sim 93\%$  of active area. This carpet has a modular structure, the basic module being a Cluster ( $5.7 \times 7.6 \text{ m}^2$ ), divided into 12 RPCs ( $2.8 \times 1.25 \text{ m}^2$  each). Each chamber is read by 80 strips of  $6.75 \times 61.8 \text{ cm}^2$ , logically organized in 10 independent pads of  $55.6 \times 61.8 \text{ cm}^2$  [1]. This digital response of the detector can be used up to energies of a few hundreds of TeV. In order to extend the dynamic range, a charge read-out has been implemented by adding to every RPC two large size pads of dimension  $140 \times 125 \text{ cm}^2$  each [2]. The central carpet, constituted by  $10 \times 13$  clusters, is enclosed by a guard-ring partially instrumented ( $\sim 40\%$ ) in order to improve rejection capability for external events. The full detector is composed by 154 clusters for a total active surface of  $\sim 6700 \text{ m}^2$ . A lead converter 0.5 cm thick will uniformly cover the apparatus in order to improve the angular resolution. The main features of the ARGO-YBJ experiment are: (1) time resolution  $\sim 1 \text{ ns}$ ; (2) space information from strips; (3) time information from pads. Due to its small size pixels, the detector is able to image the shower profile with an unprecedented granularity and with an high duty cycle ( $\approx 100\%$ ) in the typical field of view of an EAS-array ( $\sim 2 \text{ sr}$ ).

Since December 2004 the pointing accuracy of the detector has been studied with 2 different carpet areas: 42 Clusters (ARGO-42,  $\sim 1820 \text{ m}^2$ ) and 104 Clusters (ARGO-104,  $\sim 4500 \text{ m}^2$ ), yet without any converter sheet. The data have been collected with a so-called "Low Multiplicity Trigger", requiring at least 60 fired pads on the whole detector [3]. The corresponding median energy of proton-induced triggered showers is  $\approx 6$  (3.7) TeV for ARGO-42 (ARGO-104). In this paper we present a first measurement of the angular resolution of the ARGO-YBJ detector.

## II. IDENTIFICATION OF SHOWERS WITH CORE OUTSIDE THE DETECTOR

Showers of sufficiently large size will trigger the detector even if their core is located well outside its boundaries: in our case  $\sim 70\%$  of the triggering showers are external (i.e., events with core outside the detector). In order to obtain a good angular resolution it is vital to select internal showers since the direction of the showers with outer core in general is badly reconstructed due to the bending of the shower front and to the unknown core position. To find the optimal selection method we have to rely on MC calculations, thus we have simulated, via the Corsika/QGSJet code [4], proton induced showers with particle spectrum  $\propto E^{-2.75}$  ranging from 100 GeV to 1 PeV in the zenith angle interval 0-40 degrees. The detector response has been simulated via a GEANT3-based code. The core positions have been randomly sampled in an energy-dependent area large up to  $800 \times 800 \text{ m}^2$ , centred on the detector.

Any selection criterion will results in the following subcategories: accepted showers, rejected showers, falsely accepted events and falsely rejected ones. The "contamination" (C) and "efficiency" ( $\epsilon$ ) percentages can be expressed as follows:

$$C = \frac{N_{FA}}{N_{ac} - N_{FA}} \times 100\%$$

$$\epsilon = \left(1 - \frac{N_{FR}}{N_{ac} - N_{FA}}\right) \times 100\%$$

where  $N_{FA}$  is the number of falsely accepted showers,  $N_{FR}$  is the number of falsely rejected showers and  $N_{ac}$  is the total number of accepted events. The normalization is with respect to the number of showers that have been correctly accepted:  $N_{ac} - N_{FA}$ . In order to determine whether the core actually falls outside the carpet boundary, various parameters based on particle density have been studied [5], [6]. In this analysis we consider showers as internal if they satisfy the following condition: the particle density in the inner 20 (66) clusters is higher than that of the outer ring for ARGO-42 (ARGO-104) detector. The shower core positions of the selected events are hence reconstructed by means of the Maximum Likelihood Method [7]: any core lying outside the detector edge is further rejected. In Fig.1 the shower core position resolution of internal selected proton-induced events is shown for ARGO-42 and ARGO-104 carpets. The resolution worsens due to the

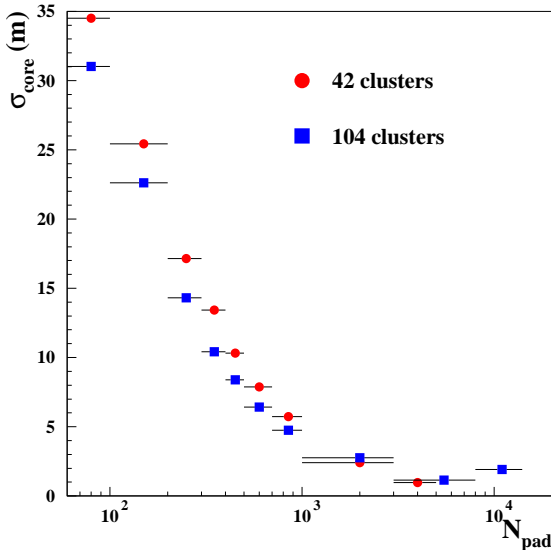


Fig. 1. Shower core position resolution of internal selected proton-induced events for ARGO-42 and ARGO-104 detectors. The error bars refer to the width of the pad multiplicity bins.

detector overflows at very large shower sizes (the total pad number is 5040 (12480) for ARGO-42 (ARGO-104)). From the figure it results that the core position is reconstructed with a resolution better than 2 m for  $N_{pad} \geq 1000$ . Moreover, from MC simulations it results that for any given multiplicity the shower core position resolution is better for  $\gamma$  than for proton-induced showers, due to the larger lateral particles spread in these latter.

As an example, for ARGO-104 the internal events selection used in this analysis gives for  $N_{pad} \geq 200$  (500) a contamination  $C=14$  (4)% and an efficiency  $\epsilon = 61$  (67)%. The median energies of these selected proton-induced events are  $\approx 4.5$  and  $\approx 10$  TeV, respectively. For lower multiplicities the contamination increases up to  $\approx 40\%$  due to the small dimension of the detectors and to the lack of the guard-ring currently under installation. The majority of the incorrectly accepted and rejected events are located near the carpets boundary, making the contamination less a concern, as the core of these events can still be located with small errors. The performance of this procedure is higher for  $\gamma$ -induced showers due to their more compact density lateral distribution.

### III. ESTIMATION OF THE ANGULAR RESOLUTION

In a search for cosmic point  $\gamma$ -ray sources with ground-based arrays the main problem is the rejection of the background due to charged cosmic rays, therefore a good angular resolution (i.e., the accuracy in estimating the arrival direction) is necessary and the identification of a firm calibration is fundamental. The angular resolution has in general two components: (i) a statistical one, due to fluctuations of the shower development and the detector noise; (2) a systematic error (i.e., the pointing error) arising from a possible misalignment of the detector, the uncertainty in the calculated shower core position or from an inaccurate shower front description. The

standard method to estimate the statistical angular resolution of an EAS array is the so-called "Chessboard Method". The pointing error, instead, can be studied by observing the shadowing effect of cosmic rays from the direction of the Moon. Other systematic errors can be investigated by means of MC simulations comparing the true and reconstructed primary directions.

In this paper we have studied the pointing accuracy of the increasing ARGO-YBJ detector with the following techniques: (1) chessboard method, which splits the detector into two parts and compares the two measured arrival directions; (2) MC simulation; (3) examination of the distribution of the arrival directions; (4) very preliminary study of the shadow of the Moon.

#### A. Analysis with the Chessboard Method

The angular reconstruction procedure has been tested with data by splitting the detector into two parts and reconstructing each event as if it were two separate events detected by the two separate sub-arrays. One detector consists of all the even-numbered pads and the other consists of all of the odd-numbered pads [8]. From a comparison of the two measured arrival directions one can derive the *statistical angular resolution* of each sub-array and then of the full detector.

The measured angle  $\psi$ , difference between the even and odd reconstructed directions, is connected to the pointing accuracy of the single sub-arrays by the relation  $\psi = \sqrt{(\Delta\theta_{true/even})^2 + (\Delta\theta_{true/odd})^2}$ , where  $\Delta\theta_{true/even,odd}$  is the angle between the true shower direction and that reconstructed with the even (or odd) sub-array.

This method is not sensitive to systematic tilts of the direction, e.g. if the fitting function does not accurately describe the shower front or if the shower core is not determined accurately, since the two reconstructed directions are affected in the same way and preferentially tilted in the same direction. The chessboard method only gives information on statistical errors and the resulting angle difference is only one component of the true angular resolution.

In this analysis the shower primary direction is reconstructed by means of an iterative procedure, with a conical correction to the shower front fixed to the value  $\alpha = 0.03$  ns/m, applied to events reconstructed inside the two carpet areas [6]. The relative time offset (due to differences in cable length, etc.) among different pads has been estimated with the method described in [9]. The analysis presented in this paper refers to showers with a zenith angle  $\theta < 40^\circ$ . We require that the difference in the number of fired pads in both sub-arrays must be less than 10%. This guarantees that both reconstructions have a similar systematical and statistical error.

In order to estimate the pointing accuracy of the detector we used the  $\psi_{72}$  parameter, a measure of the angular resolution defined as the value in the angular distribution which contains  $\sim 72\%$  of the events. This is a useful definition because, assuming that the Point Spread Function (PSF) for the entire detector is a Gaussian, it describes a solid angle which maximizes the signal from a point source on an uniform background [10].

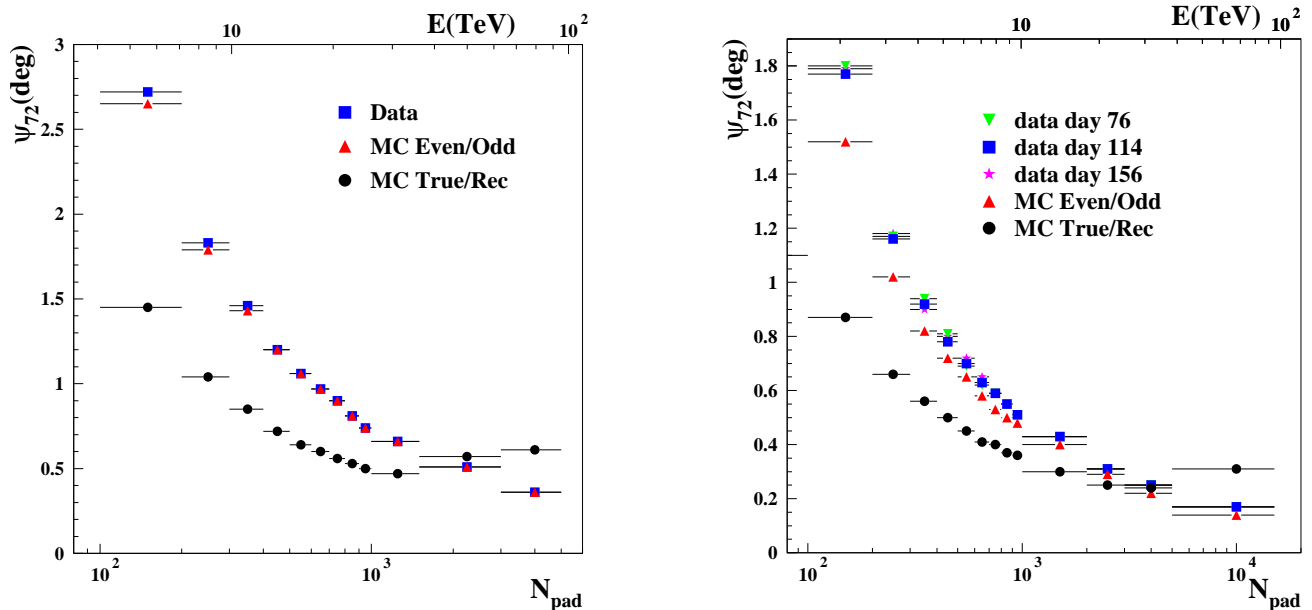


Fig. 2. The opening angle  $\psi_{72}$  measured via the Chessboard Method for ARGO-42 (left plot) and ARGO-104 (right plot) as a function of pad multiplicity, compared to MC simulation. The zenith angle of selected events is  $\theta < 40^\circ$ . In the right plot measurements performed in three different days are shown. The error bars refer to the width of the pad multiplicity bins.

The rms projected angular resolution of the detector is given by the relation  $\sigma_\theta \approx \psi_{72}/1.58$ .

In Fig.2 the opening angle  $\psi_{72}$  calculated via the chessboard method with data is compared, as a function of pad multiplicity  $N_{pad}$  (i.e., the sum of even and odd pads), to the MC simulation. We have simulated proton induced showers with particle spectrum  $\propto E^{-2.75}$  ranging from 100 GeV to 1 PeV in the uniform zenith angle interval 0-40 degrees as described in Section II. The left plot refers to ARGO-42, the right one to ARGO-104. In the right plot the  $\psi_{72}$  parameter has been calculated in three different days: the result shows the stability of the detector performance. The upper scale shows the estimated median energy of proton-induced triggered events for the different multiplicity bins. As can be seen from the plots, there is a satisfactory agreement of the simulated result with the experimental one. The  $\psi_{72}$  parameter improves roughly proportionally to  $N_{pad}^{-0.7}$  both for ARGO-42 and ARGO-104. In a shower flat temporal profile approximation, neglecting any dependence on the core position, one would expect, on a simple statistical basis, that  $\psi_{72}$  decreases as  $N_{pad}^{-0.5}$ . However, as the increased number of fired pads also means an increased shower size, and therefore an increased number of particle detected on the single pad, the intrinsic error in timing (due to the disc thickness and curvature) decreases, leading to a steeper than  $N_{pad}^{-0.5}$  diminution in the overall angle estimate.

At low multiplicity the poor agreement between data and MC is due to the high contamination of external events. In a previous work with ARGO-42 data [6] we studied the limiting capability of a RPC detector by means of a more severe selection of internal events that has granted a better agreement but with a too small efficiency ( $\epsilon \sim 10\%$ ). Studies are in

progress to identify and reject efficiently external showers with a small particles number. Anyhow, adding a 0.5 cm lead sheet on top of the RPCs will lead to an improvement of the angular resolution by a factor of at least 30% for very low pad multiplicity, even with an high contamination [11].

### B. Analysis with the MC simulation

The true shower direction of the MC events is known, therefore the angular resolution can be computed directly from the differences  $\Delta\theta_{true/rec}$  between true and reconstructed shower directions. In Fig.2 the filled circles refer to the parameter  $\psi_{72}$  calculated via MC simulations. The opening angle worsens due to the detector overflows at very large shower sizes (a behaviour similar to that of the shower core position resolution in Fig. 1). Unlike the chessboard method, the calculation of the angular resolution in this case is sensitive to the shower core position resolution and to the accuracy of the temporal profile description. As a consequence, these systematic errors can be limiting factors for  $\Delta\theta_{true/rec}$ .

If the two sub-arrays are totally independent, the angular difference between the even and odd is expected to be approximately twice the angular resolution of the entire detector:  $[\sigma_{true/rec}]/[\sigma_{even/odd}] \sim 0.5$  [12]. Firstly, one would divide the difference distribution by  $\sqrt{2}$  to get the distribution of each sub-array with respect to the true direction, due to the fact that we used two independent measurements with about the same error and the two errors added quadratically. Another factor  $\sqrt{2}$  is due to the fact that the full detector has twice as many pads as each sub-array and the angular resolution is assumed to decrease as  $N_{pad}^{-0.5}$ . As a consequence, the difference between the two directions of sub-arrays is assumed larger than that between the direction of either sub-array and the true shower

direction.

As can be seen from Fig.2, this hypothesis is not correct: a dependence of the ratio  $[(\psi_{72})_{true/rec}]/[(\psi_{72})_{even/odd}]$  on the total pad multiplicity is evident. This factor varies from  $\sim 0.5$  for very small showers to  $\sim 1$  for large showers ( $N_{pad} \sim$  few thousands). This is due to the effect of systematical errors which add quadratically to the statistical ones estimated by the chessboard method. At very low multiplicity the effect of the statistical errors is dominant and  $[(\psi_{72})_{true/rec}]/[(\psi_{72})_{even/odd}] \sim 0.5$ . When this factor is about 0.7 the systematical and statistical errors are equivalent. For greater values the systematic error is dominant. As a consequence, we have calculated with a simulation the factor by which the measured angle  $(\psi_{72})_{even/odd}$  must be multiplied to obtain the angular resolution. As an example, the *average statistical angular resolution* for the ARGO-104 detector measured with the chessboard method, up to  $\approx 4000$  fired pads, can be described by the following equation:

$$\sigma_{even/odd}(deg) = \frac{(\psi_{72})_{even/odd}}{1.58} \cdot [0.62 + 1.1 \cdot 10^{-4} \cdot N_{pad}]$$

Obviously, this measured angular resolution refers to hadron-induced air showers. From MC calculations the angular resolution for photon-induced showers results a factor of 20% lower due to their better defined temporal profile. At a pad multiplicity  $N_{pad} \sim 2000$  ( $\sim 4000$ ) for ARGO-42 (ARGO-104)  $(\psi_{72})_{true/rec} \approx (\psi_{72})_{even/odd}$ . This fact shows that the mean difference between the directions reconstructed by the two sub-arrays is similar to that between the direction of either sub-array and the true shower direction. For higher pad multiplicity the opening angle calculated via the chessboard method is significantly better than the  $(\psi_{72})_{true/rec}$  parameter, which seems to be limited by to some systematical error. Since the even-odd angle is independent of core location errors, this shows that the difficulties in accurately reconstructing the core location imply a significant portion of the error in the angular reconstruction. Calculations are in progress to evaluate the error in the determination of the shower direction induced by the uncertainty in the core determination. In fact, in order to obtain a realistic estimate of the angular resolution one has to add this error to  $\sigma_{even/odd}$ . Another probable source of systematical error may be an inaccurate shower profile description. Indeed, as it is well known, the conical slope of the shower front lowers with increasing shower size. These systematical errors affect both directions reconstructed by the sub-arrays in the same way, tilting the result in the same direction. In view of making conservative estimates of the angular resolution for  $N_{pad} \geq 2000$  (3000) we use the worse resolution, i.e. that determined via MC simulations:  $\sigma \approx 0.26^\circ$  ( $0.13^\circ$ ) for ARGO-42 (ARGO-104).

Generally, the improvement of the angular resolution with increasing apparatus area is explained in terms of increased detectors number, i.e., the opening angle of ARGO-104 is expected to be roughly a factor of  $2.5^{-0.7}$  better than that of ARGO-42, being 2.5 the ratio between ARGO-104 and ARGO-42 pads total number. However, the approximation of

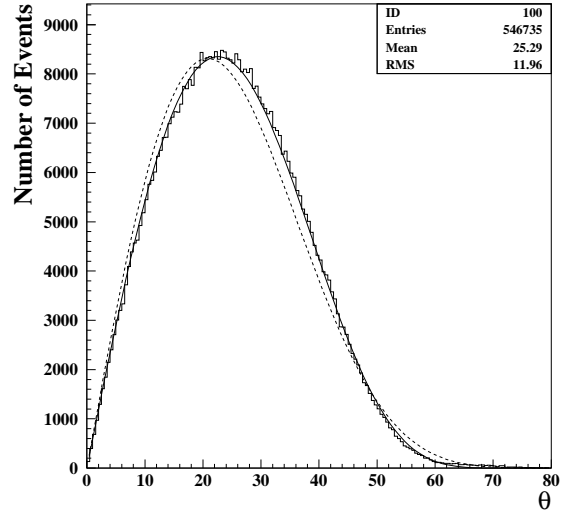


Fig. 3. Measured zenith angle distribution for internal selected events in ARGO-104. The "exponential" (solid line) and " $\cos^n\theta$ " (dashed line) best fits are also shown.

a flat lateral distribution of shower particles, neglecting any effect due to the conical shape of the temporal profile, is not correct. We studied the dependence of the angular resolution on the detector size comparing the  $\psi_{72}$  parameter at fixed fired detectors densities: i.e. comparing the opening angle calculated for ARGO-42 at a given multiplicity  $N_{pad}$  with that calculated for ARGO-104 at a corresponding multiplicity  $2.5 \cdot N_{pad}$ . From MC simulations it results that  $(\psi_{72})_{104} \approx 0.7(\psi_{72})_{42}$ , i.e., the improvement is consistent with the increase of lever arm moving from ARGO-42 to ARGO-104 (by a factor of about 1.54) and not with that of detectors number ( $2.5^{-0.7} \sim 0.53$ ).

### C. Analysis with the zenith angle distribution

In general, most of the showers should come from a zenith angle  $\theta \approx 22^\circ$  due to the folding of atmospheric absorption with the angular acceptance of the detector. In Fig.3 the measured zenith angle distribution of internal events for ARGO-104 is shown. The best fit is provided by an  $\exp(-n/\cos\theta)$  law, with  $n = \gamma x_0/\lambda = 5.361 \pm 0.005$ , where  $\gamma$  is the index of the primary energy spectrum and  $x_0$  the observation depth. The resulting absorption mean free path of showers is  $\lambda \approx 198 \text{ g/cm}^2$ , consistent with the EAS measurements [13], and the barometric effect  $\beta = \gamma/\lambda = -(\Delta n/\Delta x)/n \approx 0.9\% \text{ mbar}^{-1}$ . The difference in fitting the angular distribution with an exponential (solid line of Fig.3) or with a  $\cos^n\theta$ ,  $n = 6.90 \pm 0.01$  (dashed line) function shows that the shape is dominated by the physical effect of atmospheric absorption. Distributions dominated by instrumental effects are better fitted with  $\cos^n\theta$  behaviors [14]. The best fit curve reaches the maximum at zenith angle  $\theta \approx 22^\circ$ , while the average value is  $\langle \theta \rangle = 25.29^\circ$ . Only about 6% (0.3%) of the showers have zenith angles larger than  $45^\circ$  ( $60^\circ$ ). The direction distribution of recorded showers is centred around the zenith, and does not display features indicative of inaccurate timing. These results are in good agreement with those found for ARGO-42 [6].

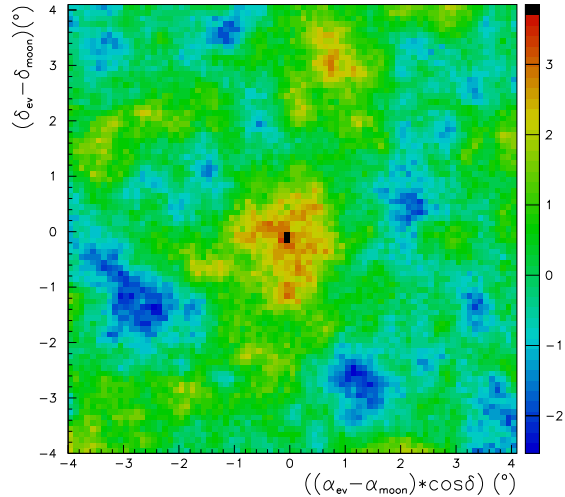


Fig. 4. Preliminary sky map of ARGO-42 around the Moon position for  $N_{pad} > 500$  and  $\theta \leq 50^\circ$ . The scale on the right indicates the statistical significance in each  $0.1^\circ \times 0.1^\circ$  bin.

#### D. Analysis with the shadow of the Moon

The analysis of the deficit of cosmic rays from the direction of the moon is a well known method to determine the angular resolution of an EAS array [15]. The primary aim of this method is to determine the orientation of the detector relative to the celestial coordinates and to investigate the systematic pointing error. From December 2004 to July 2005 ARGO-42 has been put in data taking observing the Moon for  $\sim 338.3$  h (with a duty-cycle of  $\sim 50\%$ ). A very preliminary analysis of the shadow of the Moon has been performed filling a 2-dimensional sky map around the Moon position [16]. The statistical significance of the deficit of cosmic ray events is  $\approx 4.6\sigma$  for  $N_{pad} > 60$  ( $E_{median} \approx 4$  TeV). We note that the low energy threshold and the pointing accuracy of the detector lead to a Moon shadow detection in a very short observation time. As an example, Fig.4 shows the smoothed map of the significance for showers with  $N_{pad} > 500$  ( $E_{median} \approx 20$  TeV, statistical significance of the shadow  $\approx 4\sigma$ ). Unfortunately, due to the low statistics of the sample in this analysis we were not able to perform the same selection of internal events previously discussed, therefore all triggered events have been considered. Nevertheless, in order to determine the angular resolution with this method, a least squares fit of the angular distance between the moon position and the shower reconstructed directions was made with a Gaussian distribution [17]. In Fig.5 the angular resolution of ARGO-42 detector measured with different methods is compared to MC simulations as a function of the minimum fired pads number. The low statistics limits the calculation to 500 pads and the measured angular resolution values. Nevertheless, as can be seen from the figure, the overall results are in fair agreement. The angular resolution of ARGO-42 is better than  $0.5^\circ$  for  $N_{pad} > 400$  ( $E_{median} \approx$

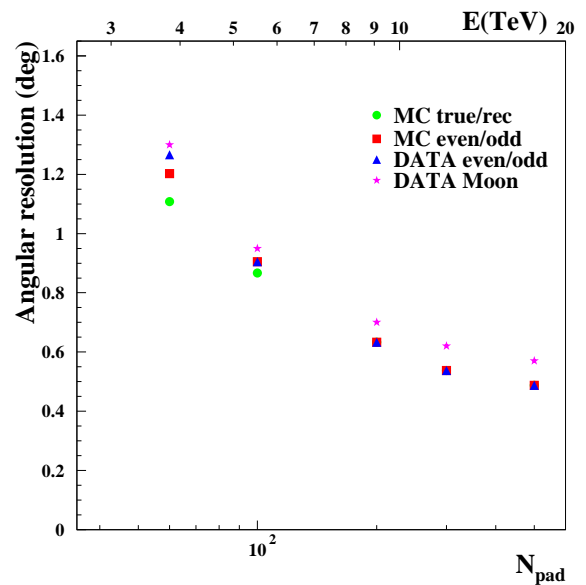


Fig. 5. Angular resolution of ARGO-42 detector measured with different methods and compared to MC simulations.

15 TeV), yet without any lead sheet on the RPCs.

#### IV. CONCLUSIONS

Since December 2004 increasing fractions of the ARGO-YBJ carpet have been put in data taking even if with a reduced duty-cycle due to installation and debugging operations. In this paper we presented a first measurement of the pointing accuracy of two different carpet areas. The capability of reconstructing the primary shower direction has been investigated with the chessboard method and with a very preliminary Moon shadow analysis. We found a good agreement between the overall results making us confident about our reconstruction algorithms. Studies are in progress to apply this analysis to the full detector (meanwhile installed) in order to determine the final angular resolution.

#### REFERENCES

- [1] G. Aielli et al., NIM **A562** 92 (2006).
- [2] P. Creti et al., 29th ICRC, Pune **8**, 97 (2005).
- [3] S. Mastroianni et al., 29th ICRC, Pune **5**, 311 (2005).
- [4] D. Heck et al., Report **FZKA 6019** Forschungszentrum Karlsruhe (1998).
- [5] L. Saggese and E. Rossi, 29th ICRC, Pune **6**, 37 (2005).
- [6] G. Di Sciascio et al., 29th ICRC, Pune **6**, 33 (2005).
- [7] G. Di Sciascio et al., Proc. 28th ICRC, Tsukuba (2003) p. 3015.
- [8] P.J.V. Eames et al, 22th ICRC, Moscow **2**, 449 (1987).
- [9] P. Bernardini et al., 29th ICRC, Pune **5**, 147 (2005).
- [10] Protheroe and R.W. Clay, Proc. ASA **5** (1984) 585.
- [11] C. Bacci et al., Astrop. Phys. **17** (2002) 151.
- [12] D.E. Alexandreas et al., NIM **A311** 350 (1992).
- [13] M. Aglietta et al., Astrop. Phys. **10** (1999) 1.
- [14] G. Cocconi, Handbuch der Physik, Vol. XLVI/1 (1961) 215.
- [15] G.W. Clark, Phys. Rev. **108**, 450 (1957).
- [16] S. Vernetto et al., 29th ICRC, Pune, **4**, 375 (2005).
- [17] D.E. Alexandreas et al., Phys. Rev. D**43**, 1735 (1991).